Piezoelectric and Electrostatic Properties of Electrospun PVDF-TrFE Nanofibers and their Role in Electromechanical Transduction in Nanogenerators and Strain Sensors

# Piezoelectric and electrostatic properties of electrospun PVDF-TrFE nanofibers and their role in electromechanical transduction in nano-generators and strain sensors.

*Francesco Calavalle, Marco Zaccaria, Giacomo Selleri, Tobias Cramer*, Davide Fabiani, Beatrice Fraboni*

F. Calavalle, Dr. T. Cramer, Prof. B. Fraboni
Department for Physics and Astronomy, University of Bologna, Viale Berti Pichat 6/2, 40127 Bologna, Italy
E-mail: tobias.cramer@unibo.it

F. Calavalle
present address: CIC nanoGUNE, Tolosa Hiribidea 76, 20018 Donostia – San Sebastian, Spain

Dr. M. Zaccaria, Dr. G. Selleri, Prof. D. Fabiani
Department of Electrical, Electronic, and Information Engineering "Guglielmo Marconi", University of Bologna, Viale del Risorgimento 2, 40098 Bologna, Italy

**Keywords:** nanogenerators, electrospinning, nanofibers, piezoelectric, triboelectric

Piezo- and ferroelectric nanofibers of the polymer poly(vinylidenefluoride) (PVDF) have been widely employed in strain and pressure sensors as well as nanogenerators for energy harvesting. Despite this interest, the mechanism of electromechanical transduction is under debate and a deeper knowledge about relevant piezoelectric or electrostatic properties of nanofibers is crucial to optimize transduction efficiency. Here we prepare PVDF-TrFE nanofibers at different electrospinning conditions. We compare macroscopic electromechanical response of fiber mats with microscopic analysis of single nanofibers performed by piezoelectric and electrostatic force microscopy. Our results show that electrospinning favors the formation of the piezoelectric β-phase in the polymer and leads directly to piezoelectric properties that are comparable to annealed thin films. However, during electrospinning the electric field is not strong enough to induce direct ferroelectric domain polarization. Instead we observe accumulation of triboelectric surface charges and trapped space charge in the polymer that explain the electret like macroscopic electromechanical response.

## 1. Introduction

1D piezo- and ferroelectric polymer nanomaterials such as nanofibers or nanopillars of poly(vinylidenefluoride) (PVDF) and its copolymer derivatives are an emerging material class that has attracted extensive attention for electromechanical transduction in the last years.[1–3] 1D nanostructures of PVDF have been prepared by anodized aluminium oxide based templates or electrospinning methods to yield nanofibers of diameters ranging from a few tens to several hundred nanometers.[3] Advances in fabrication processes have also led to control on the orientation and alignment of nanofibers. Compressive or tensile strain sensors that employ 1D piezoelectric nanofibers as active material have been demonstrated to exhibit exceptional voltage response upon mechanical deformation.[4–6] Nanofiber based electromechanical transduction has also been used in vibrational energy harvesting devices or nano-generators that convert repeated mechanical deformation into electrical energy stored on a capacitor with significant conversion efficiency.[7–11]

Several reasons are discussed in literature that explain why a 1D nanogeometry is advantageous for these applications with respect to thin-film or bulk materials. The strong surface confinement and the defined spatial direction of 1D materials have the potential to directly enhance piezoelectric properties in polymeric materials by improving piezoelectric crystallite growth and orientation[12,13] and by causing a self-poling effect[8,11,14]. At the same time, the high surface to volume ratio favours the trapping of electrostatic charge either by triboelectric contact electrification[7,15] or as a consequence of fabrication methods such as electrospinning.[16] Under deformation the trapped charges give rise to voltage and transient current generation. Such a mechanism is exploited in electret based transducers and is alternative to the piezoelectric effect.[16] Optimization of 1D nanomaterials for electromechanical transduction requires a clear understanding of the underlying mechanism. Macroscopic measurements often do not provide enough information to distinguish clearly piezo- or electret-based transduction as the response is an average made over a population of fibers in different geometries and subjected to complex 3D deformations. Therefore, characterization methods are

needed that assess piezoelectric as well as electrostatic properties at the level of single fibers. Such techniques hold the key to elucidate whether a piezoelectric or electret-based transduction mechanism is relevant for an effective electromechanical energy conversion in 1D nano-systems.

Here we investigate electrospun nanofibers of poly(vinylidenefluoride-trifluoroethylene) PVDF-TrFE by Piezoelectric Force Microscopy and Kelvin Probe Force Microscopy. Our measurements provide quantitative data about electrostatic and piezoelectric properties of single fibers such as the polarization, the longitudinal piezoelectric coefficient, the coercive field strength as well as their surface potential. We compare these results to macroscopic electromechanical response measurements obtained for random-fiber networks confined between two contact electrodes. Our findings elucidate the dominant electromechanical transduction mechanism and point to possible strategies to improve fiber based electromechancial sensors and energy-harvesting devices.

## 2. Results and Discussion

**Sample preparation and macroscopic characterizations:** PVDF-TrFE nanofibers were prepared by electrospinning at 20 kV and collected as a random mat on a grounded metallic substrate. **Figure 1a** shows the SEM image of a fiber mat. An average diameter of 420 +/- 150 nm is observed for our fabrication technique. The fiber mat X-ray diffraction pattern is compared in Figure 1b with the pattern of a PVDF-thin film sample. The latter has several peaks that correspond to different crystallographic phases. In the electrospun sample only one peak emerges at $2\Phi = 19.8°$ demonstrating the high content in the non-centrosymmetric β-phase, associated to piezoelectric and ferroelectric response. The prevalence of the β-polymorph in fibers prepared by electrospinning has been described earlier and is attributed to the strong elongation of the polymer/solution jet during the electrospinning.[17] Figure 1c and d illustrate the electromechanical characterizations done on the fiber mat. For these measurements the fiber mat was sandwiched between two aluminium foils that served as electrodes and that were connected to an oscilloscope ($R = 1M\Omega$). This capacitor structure was then placed in a mechanical tester and a load of 3.5 N was pressed against its surface and released at

a repeating rate of 4 Hz. We compared measurements done on the fiber mat and on a PVDF thin-film. For both cases the oscilloscope traces show a strong, reproducible signal upon the impact and release of the pressure. A change in polarity of the signal is observed upon pressure release and the overall integral is zero. Interestingly, the fiber mat shows a threefold increased voltage amplitude although the overall amount of ferroelectric material is reduced by over an order of magnitude. Similar increase in voltage response upon tensile or compressive strain has been reported in several devices based on PVDF-TrFE fibers and are typically assigned in the literature to the piezo- or ferroelectric properties of the fibers.[5,11,18]

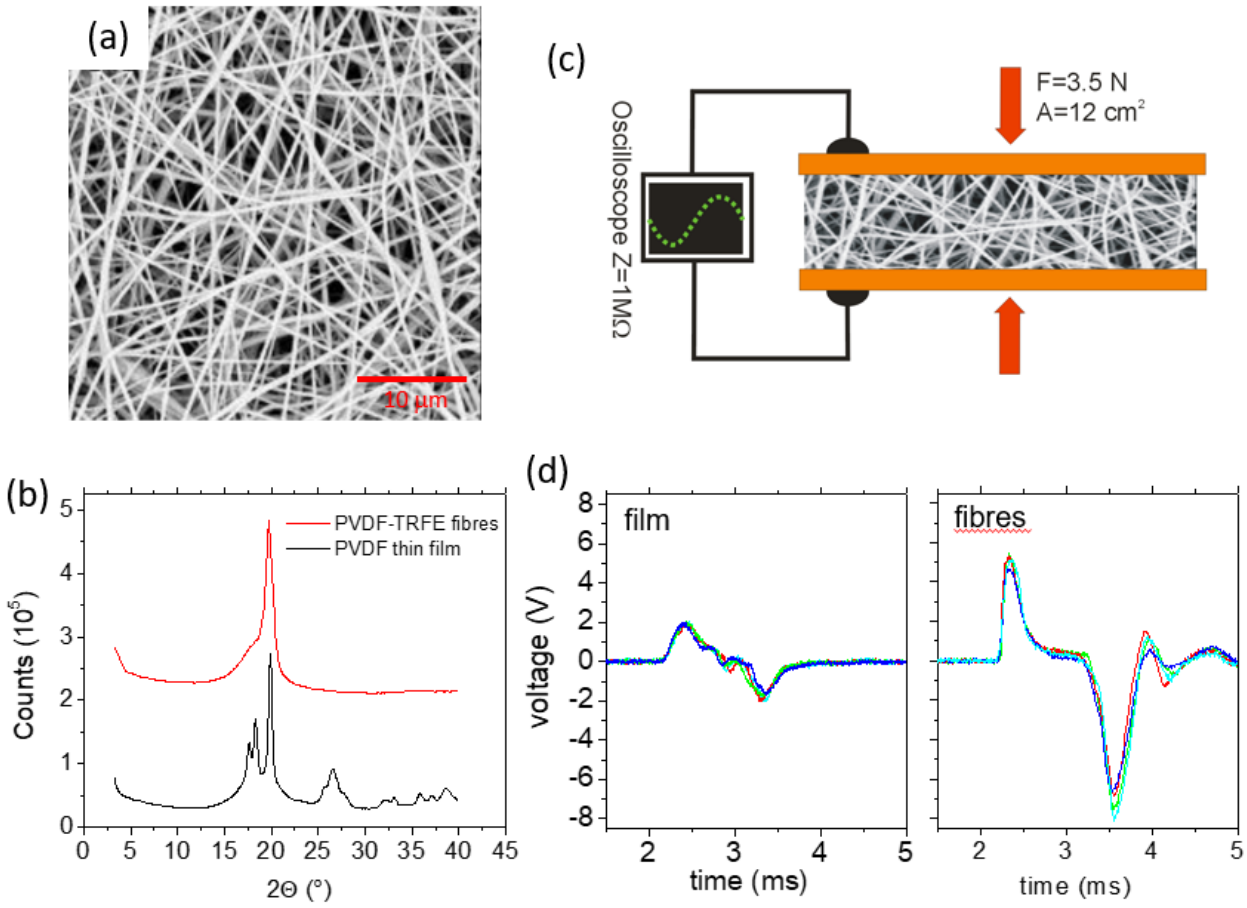


**Figure 1:** Structural and electromechanical characterization of electrospun PVDF-TrFE nanofibers mats: (a) SEM image showing the randomly positioned nano-fibers in the mat. (b) XRD spectrum with pronounced peak assigned to ferroelectric PVDF-TrFE β-phase, PVDF-film as comparison. The PVDF-TrFE spectrum was shifted upwards for clarity. (c) setup of electromechanical characterization. (d) voltage responses of thin film and electrospun fiber mats under cyclic compression.

**Piezoelectric Force Microscopy:** In order to understand the microscopic origin of the observed signal increase we investigated single PVDF-TrFE nanofibers deposited on a gold-surface with electrostatic force microscopy methods. **Figure 2a** shows typical results obtained from a PFM experiment. The height map shows a fiber of a diameter of 470 nm. On this fiber we compare positively and negatively polarized areas with an unpolarized area on the lower part of the fiber. Polarization was achieved by contacting the fiber with the grounded conductive probe at the indicated points while a strong positive or negative potential was applied for 200 ms to the gold substrate. The resulting tip induced electric field causes polarization of the fiber as evident in the maps of PFM amplitude and phase. Around the spot where a positive potential was applied, we observe a strong increase in PFM signal at phase equal to 0 demonstrating positive polarization. Laterally this polarization is confined by the borders of the nanofiber whereas along the nanofiber the polarization domain extends for around 390 nm. At the spot where a negative potential was applied instead, we observe the negative polarization that leads to a 180° phase shift. No PFM signal (low amplitude, random phase) is observed on the lower part of the fiber that was not subjected to polarization by strong tip induced electric fields. The absence of a native polarization in electrospun fibers is confirmed by measurements on several fibers deposited at positive as well as negative electrospinning voltages (see Suppl. Mat.).

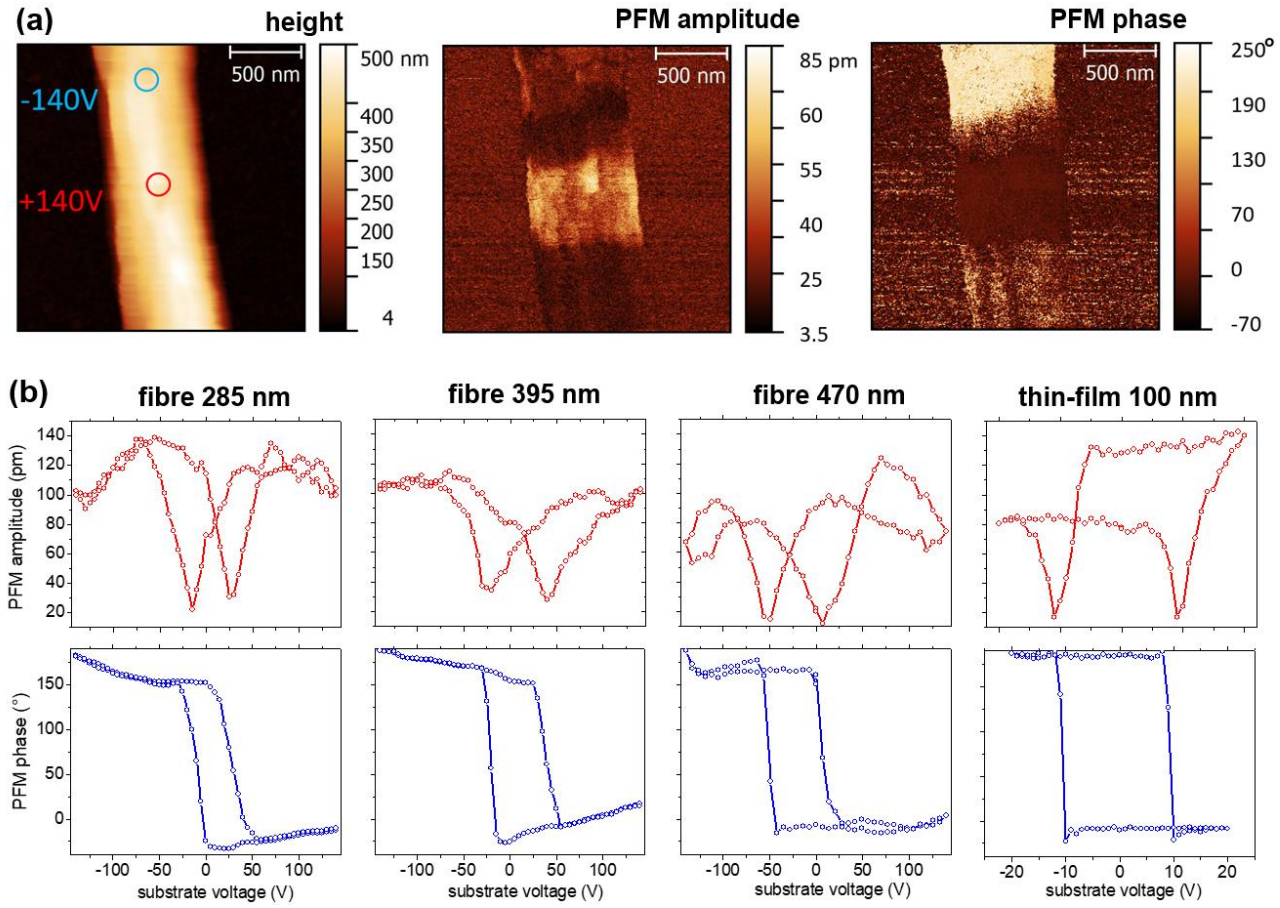


**Figure 2:** Piezoelectric force microscopy (PFM) on electrospun PVDF-TrFE fibers. (a) maps of surface height, PFM amplitude and PFM phase of a fiber after polarization at +140 V and at -140 V applied to the substrate with the tip positioned as indicated in the height map. The measurements show that fibers deposited by electrospinning were not polarized. (b) Polarization hysteresis curves of fibers of different diameter and of thin film as measured by PFM switching spectroscopy. The magnitude of the piezoelectric oscillation and the phase are shown.

In a next step we perform PFM switching spectroscopy (PFM-SS) to obtain a more detailed characterization of single fiber polarization switching. Importantly, in PFM-SS the piezoelectric response is measured in the absence of tip or substrate voltage and only after a voltage pulse of defined duration was applied to the thin film.[19] In this way artefacts due to electrostatic force induced tip indentation (recently described as converse flexoelectric response) are excluded (see Supp. Inf. Figure S3).[20] Figure 2b contains PFM-SS hysteresis loops of amplitude and phase measured on fibers of different diameter. The results are compared to a measurement done on a 100 nm thick PVDF-TrFE thin-film. All hysteresis curves show clear polarization switching causing a 180° phase shift and a

minimum in PFM amplitude. A closer look at the PFM phase shows also that the longitudinal piezoelectric coefficient $d_{33}$ has a negative sign: At negative substrate voltage, when the piezoelectric polarization (pointing out of the substrate) and the tip induced electric field are parallel, a 180° PFM phase signal is detected. Instead at positive substrate voltages the polarization and the electric field are antiparallel and the PFM phase signal is at 0°. This observation demonstrates that longitudinal piezoelectric contraction occurs if polarization and electric field are pointing into the same direction. This unusual effect leading to the negative sign of the piezoelectric coefficient is a typical signature of PVDF piezoelectric response.[21] We note that the effect is not observed in normal PFM hysteresis loops where the DC field causes strong tip-indentation (see Suppl. Fig. S3).

By comparing the PFM hysteresis loops for fibers of different diameter we note further that the increasing fiber diameter requires larger voltage to induce polarization reversal and voltages up to 50 V have to be applied to the substrate. In comparison, the polarization curve of the thin film shows similar features but contains less fluctuations in amplitude and phase. This is associated to the reduced thickness of the thin film. Also, we note in the thin-film that positive and negative polarization are characterized by different PFM amplitudes. Such an effect points to incomplete polarization reversal due to strong surface interactions.[22] In nanofibers instead the asymmetry is not observed.

From PFM switching spectroscopy experiments we extract the longitudinal piezoelectric coefficient $d_{33} = A/V_{AC,tip}$ from the PFM amplitude $A$ measured at 0 V substrate bias and AC tip bias $V_{AC,tip}$ = 3 V. The coercive potential $V_C$ is calculated from the PFM phase signal as the average substrate voltage at which the signal crosses 90° phase. Values for $d_{33}$ and $V_C$ as a function of the fiber diameter or thin-film thickness are presented in **Figure 3**. For $d_{33}$ no significant dependence on fiber diameter is observed and we calculate an average value of $d_{33}$ = -18 ± 4 pm/V. In comparison the thin film results in a slightly larger value of -22 ± 3 pm/V. Regarding the coercive potential $V_C$ we observe a dependence on fiber diameter. We approximate the behavior by assuming a linear relationship and calculate the average coercive field as $E_C = V_C$ /h where $h$ is the fiber diameter or film thickness. For

the nanofibers we obtain $E_C$ = 50 ± 16 MV/m and for the thin-film $E_C$ = 41 ± 8 MV/m. In Figure 3 we present these average values as dashed lines.

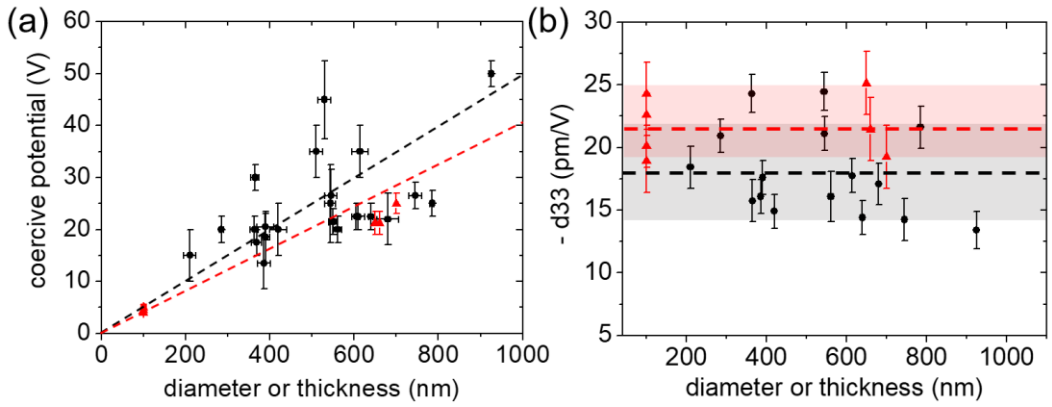


**Figure 3:** Impact of fiber diameter on piezoelectric and ferroelectric properties: (a) coercive potential as a function of fiber diameter. (b) piezoelectric coefficient $d_{33}$ as a function of fiber diameter. For comparison the values obtained on PVDF-TrFE thin films of different thickness are included (red). Straight lines represent linear fits to the data.

The PFM measurements point to two important findings: First the fibers do not show a polarization that is orthogonal to the substrate. This means that although a strong electric field is present during our electrospinning procedure, the field is not sufficient to align the dipoles of the ferroelectric domains. In typical electrospinning experiments the distance between collector and tip is several centimeters leading to electric fields on the order of 0.05-0.2 MV/m (see Supp. Fig. S4). This is orders of magnitudes below the measured coercive field needed to polarize PVDF-TrFE nanofibers. Absence of polarization in electrospun PVDF-TrFE fibers has also been confirmed in other works in the literature by second harmonic generation spectroscopy.[23] We note that our measurements cannot exclude a possible polarization in the direction of the fiber. In certain fiber-based electromechanical transducers such a polarization was discussed as a relevant mechanism.[24]

Second, the nanofibers show piezoelectric properties comparable to the thin film confirming the nano-confinement induced ß-phase crystallite formation.[25] Even without annealing, the electrospun fibers show a significant longitudinal piezoelectric coefficient of $d_{33}$ = -18 ± 4 pm/V that remains however

below the PVDF-TrFE bulk value of -31.4 V/pm.[21] Instead the $d_{33}$ is comparable to other values reported in literature for PVDF-TrFE thin films that were affected by interface clamping effect.[26] The measured coercive field of $E_C$ = 50 ± 16 MV/m is well in the range of literature values found for PVDF-TrFE films of 50 – 80 MV/m.[27] The small impact of the nano-confinement on piezoelectric properties is also in agreement with measurements on Curie transition in PVDF-TRFE nanofibers that did not show a significant shift with respect to bulk behavior.[28]

**Kelvin Probe Force Microscopy:** KPFM measures the local surface potential on a grounded conducting substrate at nanometer resolution. Variations in $V_{SP}$ are related to work-function changes in the substrate material or trapped charge present in dielectric layers on top of the conducting substrate. **Figure 4a and b** present such KPFM scans done on a sample of single PVDF-TrFE fibers shortly after their deposition by electrospinning on a grounded gold surface. The height map shows the normal fiber morphology with diameters in the range of a few hundred nanometers. In the $V_{SP}$ map we observe that the fibers have a more negative $V_{SP}$ than the gold surface. In addition, in the large area scan (Figure 4a) one notes two fiber segments with a significantly more negative $V_{SP}$ reaching -2 V. The high-resolution scan of such a segment (Figure 4b) shows how the $V_{SP}$ changes on the surface of the single fiber. In particular, one notes more negative potential at the sidewall of the fiber. We performed such measurements on several fibers of this sample to calculate an average $V_{SP}$ and a standard deviation. This procedure was repeated on fibers produced with positive electrospinning voltages and on an unpolarized PVDF-TrFE thin film. These measurements were repeated after 80 and 150 days of storage under ambient conditions. The resulting graph is presented in Figure 4c. We make two important observations: First, fibers deposited by positive electrospinning potential as well as the thin film produced by spin coating possess a constant negative $V_{SP}$ of -0.4 +/- 0.1 V. This $V_{SP}$ is not significantly changed during storage. Second, the fibers produced with a negative electrospinning voltage exhibit a much lower average $V_{SP}$ when measured shortly after the deposition. During storage the $V_{SP}$ increases and reaches the value observed in thin films.

We explain the observations by the trapping of negative charge on the nanofibers following two different mechanisms. First, a generally negative $V_{SP}$ on PVDF-TrFE surfaces is explained by triboelectric contact electrification. Fluorinated polymers are generally positioned at the lower bottom of the triboelectric series due to the strongly electron attracting properties of the fluorine atoms. Accordingly, PVDF-TrFE binds electrons when it gets into contact with other materials positioned higher in the triboelectric series. As fibers are on top of a metal layer, the surface charge is screened by positive image charges in the metal electrode. The resulting interfacial dipole shifts the surface potential measured in KPFM and hence the measured $V_{SP}$ characterizes the triboelectric surface charge. The triboelectric mechanism is effective in fibers as well as thin films and causes $V_{SP}$ values of -0.4 V.[29] The second mechanism explains the much more negative $V_{SP}$ observed only at negative electrospinning potentials by ionization charges that are introduced by the strong electric field present at the electrospinning needle. Although the fibers are collected on a conductive surface, the migration of the trapped negative ionization charge is slow and relaxation into an equilibrated electrostatic condition can take several days. At positive electrospinning voltage a similar charging is not observed likely because positive ionic charges have higher mobility in PVDF-TrFE fibers and thus migrate to the ground electrode on much shorter time-scales. This explanation is corroborated by the data shown in Figure 4d where we plot the $V_{SP}$ of charged fibers as a function of fiber diameter. The linear fit of the data demonstrates that there is a trend that relates thicker fibers to more pronounced charge trapping as would be expected for a kinetically trapped space charge.

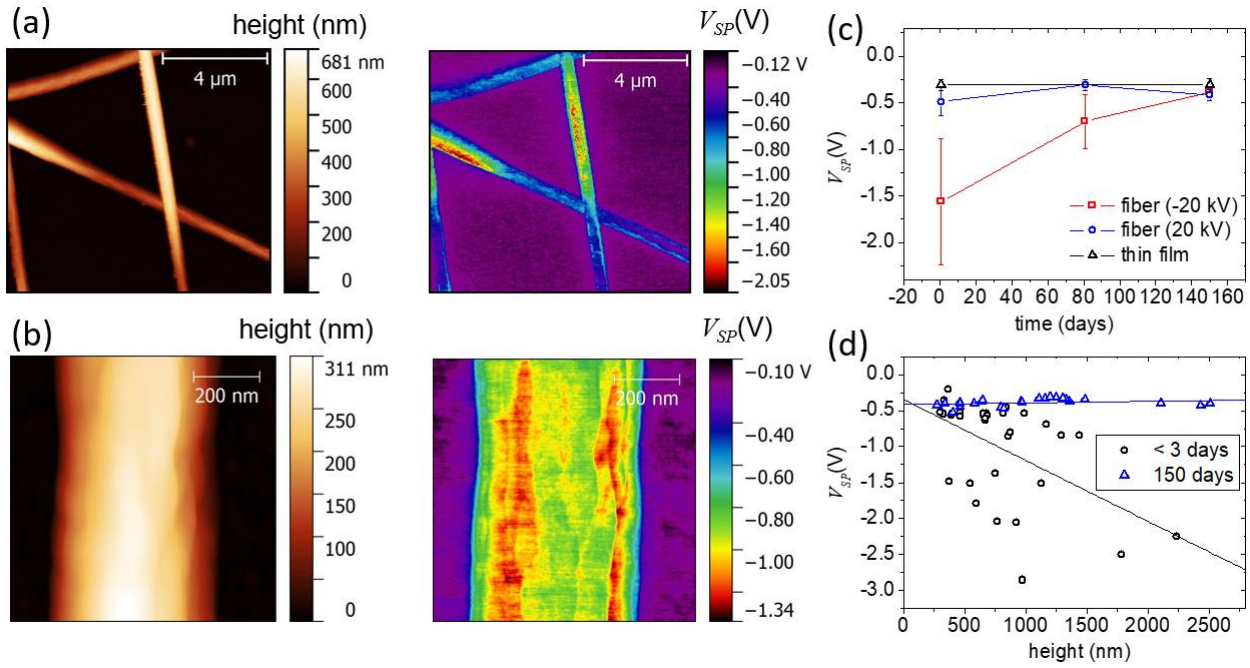


**Figure 4:** Scanning Kelvin Probe Microscopy to determine nanofiber charging: (a,b) height and surface potential ($V_{SP}$) images of nanofibers deposited on gold; (c) average $V_{SP}$ and standard deviation of $V_{SP}$ measured on nanofibers and thin film as a function of storage time after deposition; (d) $V_{SP}$ as a function of fiber diameter for samples characterized shortly after electrospinning (black) or after 150 days of storage (blue). Lines represent linear fits to the data.

## 3. Discussion

The results we have obtained about the single nanofiber piezo- and electrostatic properties allows us to draw important conclusions on the macroscopic electromechanical response of nanofiber mats. In **Figure 5a** we show three possible mechanisms that lead to electret behaviour and introduce electrostatic charge in nanofiber samples. Our measurements point out that only two of them are relevant for the here investigated sample: one is based on triboelectric contact electrification and the other on trapped space charges introduced by the electrospinning procedure. The latter is only temporary present as on longer time scales the charges migrate out of the PVDF-TrFE polymer material. A third mechanism to introduce electrostatic charge could be based on the polarization of ferroelectric domains. However, electric fields present in electrospinning were not strong-enough to induce this polarization in the direction orthogonal to the fiber. Also, one has to consider that the coercive field of the fibers is above the air dielectric breakdown. Therefore, polarization of PVDF-

TrFE fiber networks would need a strong dielectric matrix to avoid dielectric breakdown. If this can be achieved, we predict improved charge accumulation and hence a performance increase in fiber based nano-generators.

Once the PVDF-TrFE fibers behave as charged electret, a displacement current is generated when interacting with electrodes as shown in Figure 5b. Important for efficient electrostatic transduction is the asymmetry between the electrodes. The bottom electrode should remain in close contact with fibers while the top electrode should vary in distance depending on the applied strain. In randomly deposited fiber mats such an asymmetry is generated as the deposition starts on a flat surface. With increasing amount of fibers the roughness increases following a Poissonian statistics. For this reason, the top surface of the fiber mat exhibits a different surface morphology and we observe the strong voltage signals when two contacting electrodes compress the fibre mat as shown in Figure 1. We note that more efficient methods to enhance the electrode asymmetry such as compressible cylindrical cavities are described in the literature.[9]

The second mechanism able to generate a displacement current, shown in Figure 5b, relies on a direct piezoelectric effect in which compressive strain acts directly on the fiber contacted by to electrodes to produce the voltage and current response. Here we exclude this effect for two reasons: First the deposited fibers analysed in this paper are not polarized. Contributions from different piezoelectric domains would cancel. Second, the sparse network of the fiber mat accommodates macroscopic compressive strain by network deformations and fiber bending. Compression on the single fiber level could be unlikely to occur.

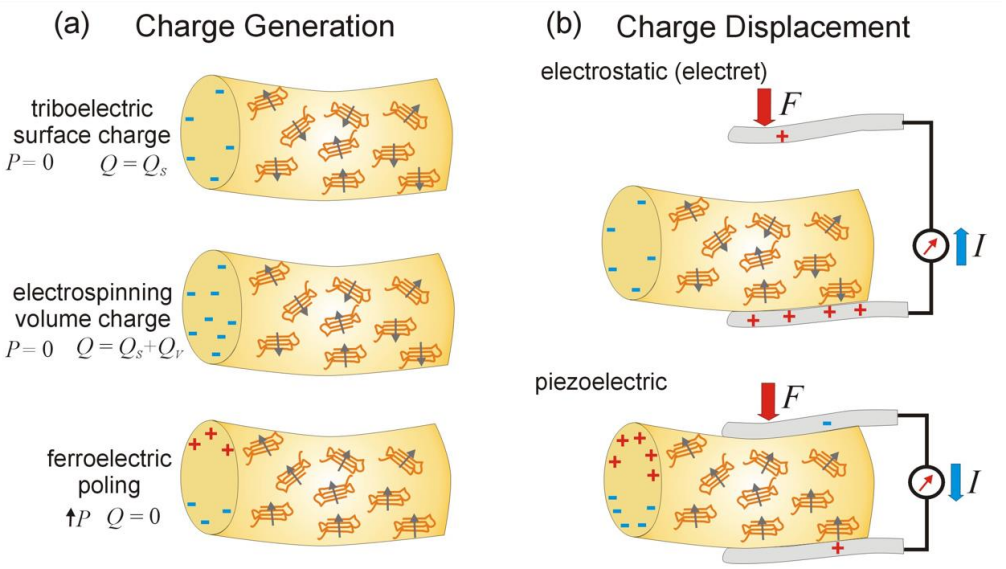


**Figure 5:** Electromechanical transduction with piezo- and ferroelectric nanofibers. (a) The scheme shows different mechanisms that cause charge in fibers such as (i) accumulation of triboelectric surface charges, (ii) presence of trapped charges in the volume as a consequence of electrospinning or (iii) poling of ferroelectric domains. (b) The scheme shows how a force F can be transduced into a macroscopic displacement current either due to (i) electrostatic interactions that cause displacement currents in electrodes or due to (ii) direct piezoelectric effect. Here we argue that the former mechanism is the most relevant one for electrospun PVDF-TrFE nanofibers based transducers.

## 4. Conclusions

In conclusion, we present here a detailed microscopic characterization of single PVDF-TrFE nanofibers prepared by electrospinning. Fibers show a diameter of 420 ± 150 nm and have a longitudinal piezoelectric coefficient of $d_{33}$ = -18 ± 4 pm/V and a coercive field strength of $E_C$ = 50 ± 16 MV/m as determined by PFM switching spectroscopy. The piezoelectric properties are comparable to annealed thin films of the same material. Kelvin Probe force microscopy further demonstrates that electrospinning accumulates negative space charge in the fibers. In addition, contact electrification with the metal electrode induces a negative triboelectric surface charge. Both charges contribute to a negative electrostic surface potential and lead to electret behaviour of electrospun fibers. Consequently, we deduce that the electret response is the main cause for the observed strong electromechancial transduction in nanogenerators or strain sensor based on random electrospun fiber-mats. We exclude direct piezoelectric contributions as we could not detect any

polarization in the deposited fibers. Only stronger AFM tip-induced electric fields were able to align piezo- and ferroelectric domains. This finding points to the possibility of increasing transduction performance in macroscopic fiber mats by achieving a macroscopic polarization in an additional poling step or by increasing significantly field strength during electrospinning, since typical electrospinning fields are not able to provide an effective polarization of dipolar domains. The polarization would contribute to an electret-based transduction as the oriented ferroelectric domains would introduce an additional strong dipolar charge.

## 5. Experimental Section

*Electrospinning:* A solution of 15% w/v PVDF-TrFE (75/25 mol%, Mw=410 kDa, Solvay Specialty Polymers, Italy) in Acetone:Dimethyl sulfoxide (70:30 v/v) was electrospun (Spinbow Lab Unit) at a flow rate of 1 ml/h, a needle-to-collector distance = 17.5 cm and voltage bias of +20 kV or -20 kV. The electrospinning process was carried out at room temperature and relative humidity of about 30%. Fibers were deposited on ITO coated glass slides, Gold coated glass slides or doped silicon with 200 nm of thermal oxide. Fiber mats of 3 cm x 4 cm and about 100 μm thickness were manufactured for macroscopic electromechanical characterization.

*Thin film fabrication:* A PVDF film microstructured into areas of thickness 80-100 nm and 650-700 nm was prepared by a soft-lithography method described in literature.[30]

*Fiber mat characterization:* SEM was performed with a (PHENOM PROX Desktop SEM). Fiber diameter distribution was evaluated with PHENOM Fibermetric software. XRD was carried out with CuKα radiation source in reflection mode using a X'Pert diffractometer (PANalytical) equipped with a fast X'Celerator detector; step 0.1°, 150 s /step. For electromechanical characterization, electrospun mats of ca. 150 μm thickness were sandwiched between aluminum-foil electrodes and subjected to cyclic mechanical stress at 4 Hz repetition frequency using a mechanical tester with an electrically isolated piston made out of Teflon. The aluminium foils had an area of 30 x 40 mm leading to an

overall capacitance of 0.6 nF of the test structure. The electrodes were connected to an oscilloscope with 1 MΩ input impedance.

*Atomic Force Microscopy:* AFM experiments were performed on a NX10 system from Park-Systems, Korea. For PFM a conductive diamond coated probe (CDT-CONTR, Nanosensors, k = 0.5 N/m) was operated in contact mode at a setpoint of ca. 4 nN. Tip voltage was modulated at 3V amplitude at 17 kHz and the resulting cantilever oscillation was amplified with a lock-in amplifier to provide the PFM amplitude and phase signal. For switching spectroscopy measurements we used a Keysight B2912 source measure unit to apply short voltage pulse to the substrate surface (see Supp. Inf. Figure S2). The oscillation amplitude in units of pm was calculated using the cantilever sensitivity of 19.9 +/- 0.1 V/um as measured on a rigid silicon substrate. KPFM measurements we used a PPP-NCST-Au probe (Nanosensors, k=7.4 N/m) following measurement procedures as described in literature.[31]

**Supporting Information** ((delete if not applicable))
Supporting Information is available from the Wiley Online Library or from the author.

**Acknowledgements**
The authors thank Oliviero Bocchi and Marco Speranza for support in nanofiber characterization and discussion. BF and TC acknowledge financial support from the project "Novel smart and sustainable textiles for creative made-in-Italy design (TEX-STYLE)" financed by the Italian Government under the PON-MUIR 2018 initiative. MZ, GS and DF acknowledge financial support from the project "Smart Composite Laminates" of the Italian PRIN 2015 funding scheme.

Received: ((will be filled in by the editorial staff))
Revised: ((will be filled in by the editorial staff))
Published online: ((will be filled in by the editorial staff))

## References


[1] S. Crossley, S. Kar-Narayan, *Nanotechnology* **2015**, *26*, 344001.

[2] V. Cauda, G. Canavese, S. Stassi, *J. Appl. Polym. Sci.* **2015**, *132*, 1.

[3] L. B. Huang, W. Xu, J. Hao, *Small* **2017**, *13*, 1.

[4] Y. Jiang, L. Gong, X. Hu, Y. Zhao, H. Chen, L. Feng, D. Zhang, *Polymers (Basel).* **2018**, *10*, 1.

[5] L. Persano, C. Dagdeviren, Y. Su, Y. Zhang, S. Girardo, D. Pisignano, Y. Huang, J. A. Rogers, *Nat. Commun.* **2013**, *4*, 1610.

[6] S. H. Park, H. B. Lee, S. M. Yeon, J. Park, N. K. Lee, *ACS Appl. Mater. Interfaces* **2016**, *8*, 24773.

[7] S. Wang, Z. L. Wang, Y. Yang, *Adv. Mater.* **2016**, *28*, 2881.

[8] Y. K. Fuh, S. Y. Chen, J. C. Ye, *Appl. Phys. Lett.* **2013**, *103*, DOI 10.1063/1.4813909.

[9] J. Gui, Y. Zhu, L. Zhang, X. Shu, W. Liu, S. Guo, X. Zhao, *Appl. Phys. Lett.* **2018**, *112*, DOI 10.1063/1.5019319.

[10] Y. Wang, C. Zhu, R. Pfattner, H. Yan, L. Jin, S. Chen, F. Molina-Lopez, F. Lissel, J. Liu, N. I. Rabiah, Z. Chen, J. W. Chung, C. Linder, M. F. Toney, B. Murmann, Z. Bao, *Sci. Adv.* **2017**, *3*, 1.

[11] R. A. Whiter, V. Narayan, S. Kar-Narayan, *Adv. Energy Mater.* **2014**, *4*, 1.

[12] Y. Y. Choi, P. Sharma, C. Phatak, D. J. Gosztola, Y. Liu, J. Lee, B. Lee, J. Li, A. Gruverman, S. Ducharme, S. Hong, *ACS Nano* **2015**, *9*, 1809.

[13] Y. Wu, Q. Gu, G. Ding, F. Tong, Z. Hu, A. M. Jonas, *ACS Macro Lett.* **2013**, *2*, 535.

[14] V. Sencadas, C. Ribeiro, I. K. Bdikin, A. L. Kholkin, S. Lanceros-Mendez, *Phys. Status Solidi Appl. Mater. Sci.* **2012**, *209*, 2605.

[15] X. Chen, M. Han, H. Chen, X. Cheng, Y. Song, Z. Su, Y. Jiang, H. Zhang, *Nanoscale* **2017**, *9*, 1263.

[16] M. Zaccaria, D. Fabiani, J. Belcari, O. Bocchi, A. Zucchelli, T. Cramer, B. Fraboni, *IEEE Conf. Electr. Insul. Dielectr. Phenom.* **2016**, 137.

[17] J. S. Andrew, D. R. Clarke, *Langmuir* **2008**, 670.

[18] Y. Calahorra, R. A. Whiter, Q. Jing, V. Narayan, S. Kar-Narayan, *APL Mater.* **2016**, *4*, DOI 10.1063/1.4967752.

[19] S. Jesse, B. J. Rodriguez, S. Choudhury, A. P. Baddorf, I. Vrejoiu, D. Hesse, M. Alexe, E. A. Eliseev, A. N. Morozovska, J. Zhang, L. Q. Chen, S. V. Kalinin, *Nat. Mater.* **2008**, *7*, 209.

[20] A. Abdollahi, N. Domingo, I. Arias, G. Catalan, *Nat. Commun.* **2019**, *10*, 1.

[21] I. Katsouras, K. Asadi, M. Li, T. B. Van Driel, K. S. Kjær, D. Zhao, T. Lenz, Y. Gu, P. W. M. Blom, D. Damjanovic, M. M. Nielsen, D. M. De Leeuw, *Nat. Mater.* **2016**, *15*, 78.

[22] Y. Kim, W. Kim, H. Choi, S. Hong, H. Ko, H. Lee, K. No, *Appl. Phys. Lett.* **2010**, *96*, 012908.

[23] D. Farrar, K. Ren, D. Cheng, S. Kim, W. Moon, W. L. Wilson, J. E. West, S. M. Yu, *Adv. Mater.* **2011**, *23*, 3954.

[24] F. Mokhtari, J. Foroughi, T. Zheng, Z. Cheng, G. M. Spinks, *J. Mater. Chem. A* **2019**, *7*, 8245.

[25] Y. M. Yousry, K. Yao, S. Chen, W. H. Liew, S. Ramakrishna, *Adv. Electron. Mater.* **2018**, *4*, 1.

[26] S. Chen, K. Xao, F. E. Hock Tay, L. L. Shan Chew, *J. Appl. Polym. Sci.* **2010**, *116*, 3331.

[27] R. C. G. Naber, P. W. M. Blom, A. W. Marsman, D. M. De Leeuw, *Appl. Phys. Lett.* **2004**, *85*, 2032.

[28] A. Serghei, J. L. Lutkenhaus, D. F. Miranda, K. McEnnis, F. Kremer, T. P. Russell, *Small* **2010**, *6*, 1822.

[29] H. Choi, J. Hong, K. No, *Appl. Phys. Lett.* **2012**, *101*, DOI 10.1063/1.4734870.

[30] T. Lenz, D. Zhao, G. Richardson, I. Katsouras, K. Asadi, G. Glaßer, S. T. Zimmermann, N. Stingelin, W. S. C. Roelofs, M. Kemerink, P. W. M. Blom, D. M. De Leeuw, *Phys. Status Solidi Appl. Mater. Sci.* **2015**, *212*, 2124.

[31] T. Cramer, L. Travagli, S. Lai, L. Patruno, S. De Miranda, A. Bonfiglio, P. Cosseddu, B. Fraboni, *Sci. Rep.* **2016**, *6*, 38203.

Ferroelectric nanofibers are prepared by electrospinning of the polymer PVDF-TrFE. Piezoelectric and electrostatic properties of single nanofibers are investigated by force microscopy methods. The findings reveal the electromechanical transduction mechanism in fiber network based nanogenerators and strain sensors.

**1D Nanomaterials for electromechanical transduction**

Francesco Calavalle, Marco Zaccaria, Oliviero Bocchi, Tobias Cramer*, Davide Fabiani, Beatrice Fraboni

**Piezoelectric and electrostatic properties of electrospun PVDF-TRFE nanofibers and their role in electromechanical transduction in nano-generators and strain sensors.**

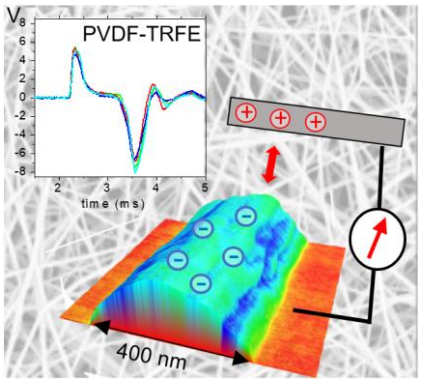

# Supporting Information

**Piezoelectric and electrostatic properties of electrospun PVDF-TrFE nanofibers and their role in electromechanical transduction in nano-generators and strain sensors.**

*Francesco Calavalle, Marco Zaccaria, Giacomo Selleri, Tobias Cramer*, Davide Fabiani, Beatrice Fraboni*

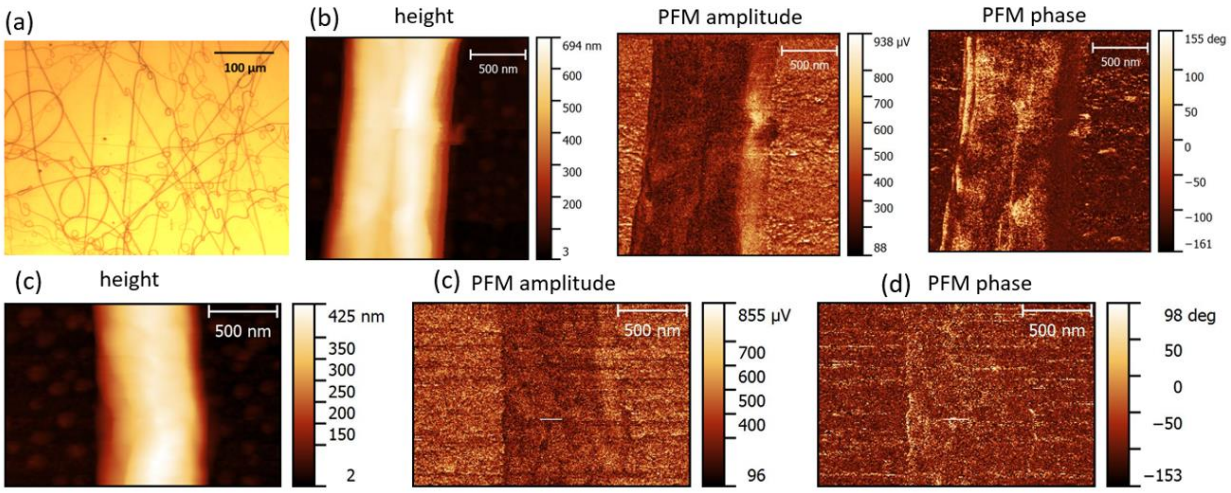


**Figure S1:** PFM investigation of electrodeposited fibers. (a) Optical microscopy image of measurement sample containing nanofibers deposited on gold surface. (b) PFM height, amplitude and phase image of fibre deposited at +20kV electrospinning potential. (c) same as (b) but fiber deposited at -20kV electrospinning potential.

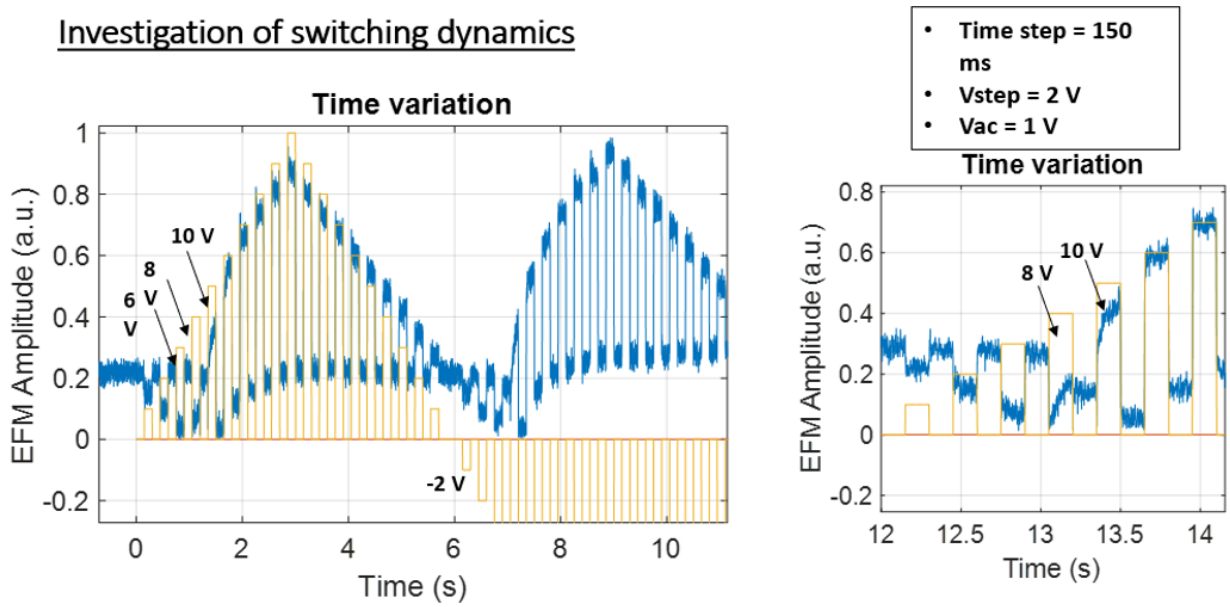


**Figure S2:** Implementation of PFM switching spectroscopy. The red line shows the potential applied to the substrate. Voltage pulses of 150 ms duration are alternated with connection to ground. The blue line show the PFM amplitude measured with the PSPD and lockin amplifier of the AFM electronics. Here polarization switching is observed at 8 V.

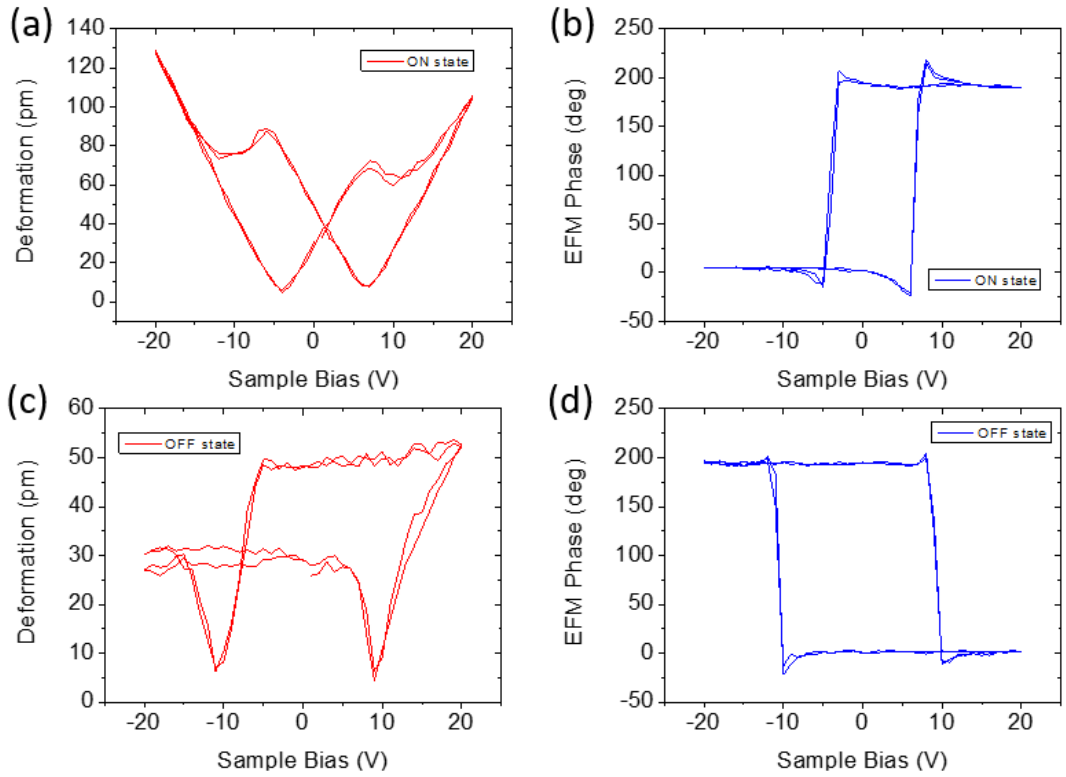


**Figure S3:** Artefacts in PVDF-TRFE thin film PFM hysteresis loop measurements. (a,b) PFM amplitude and phase measured with normal PFM hysteresis loop measurement. The DC potential is constantly applied to the sample. (c,d) PFM amplitude and phase obtained with switching spectroscopy. The DC potential is only applied in a short writing pulse. The PFM measurement is done afterwards in the absence of an external field.

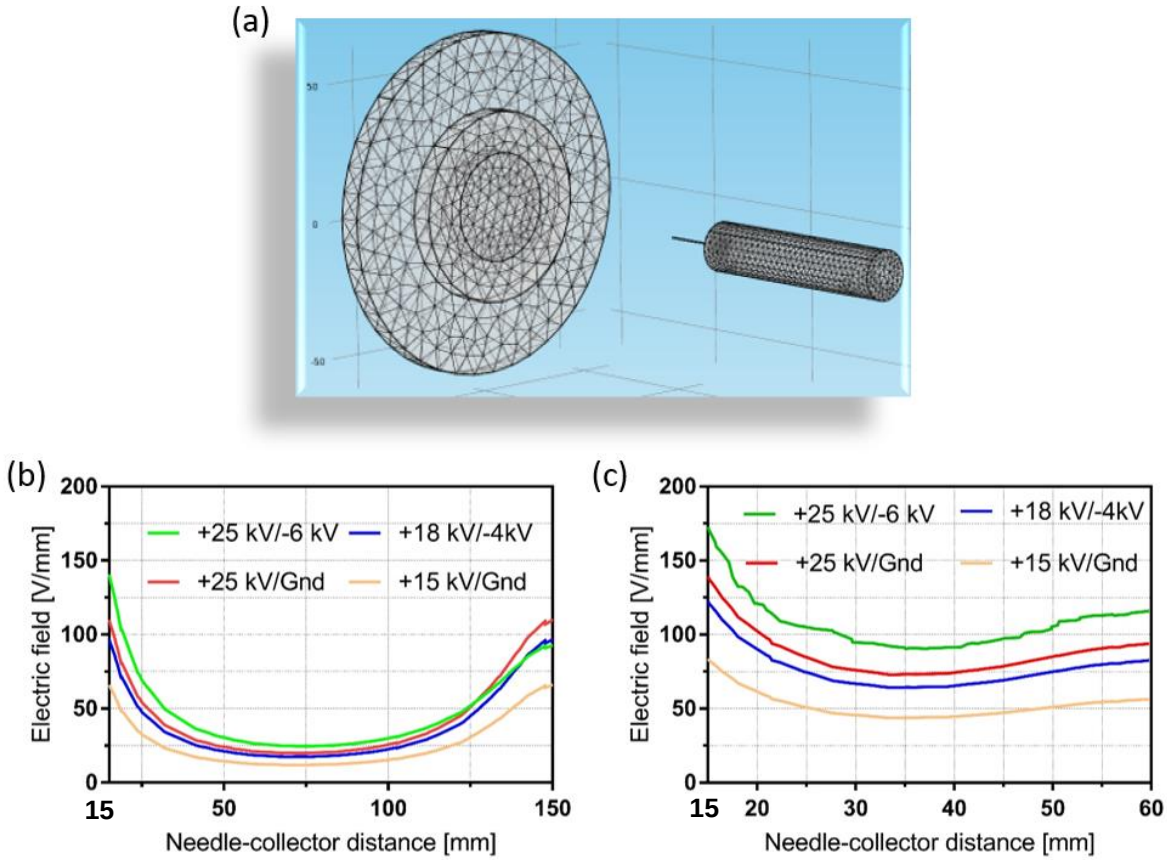


**Figure S4:** Finite element simulation of electric field during electrospinning. (a) scheme of geometry of needle and collector. (b,c) Electric field in the gap between 15 mm from the needle and collector at 150 mm (b) and 60 mm (c) distance varying the voltage applied to needle and collector. Needle voltages of 15 kV, 18 kV and 25 kV and collector voltages of 0 V (ground), -4 kV and -6 kV are considered in the simulations.